



Magnetic properties experiments and the Surface Stereo Imager calibration target onboard the Mars Phoenix 2007 Lander: Design, calibration, and science goals

K. Leer,¹ P. Bertelsen,¹ C. S. Binau,¹ L. Djernis Olsen,¹ L. Drube,¹ T. V. Falkenberg,¹ M. P. Haspang,¹ M. B. Madsen,¹ M. Olsen,¹ H. Sykulska,² S. Vijendran,² W. T. Pike,² U. Staufer,³ D. Parrat,³ M. Lemmon,⁴ M. H. Hecht,⁵ C. T. Mogenssen,⁵ M. A. Gross,⁵ W. Goetz,⁶ J. Marshall,⁷ D. Britt,⁸ P. Smith,⁹ C. Shinohara,⁹ P. Woida,⁹ R. Woida,⁹ R. Tanner,⁹ R. Reynolds,⁹ and A. Shaw⁹

Received 17 October 2007; revised 27 March 2008; accepted 29 May 2008; published 7 October 2008.

[1] The first NASA scout mission to Mars, Phoenix, launched 4 August will land in the northern part of Mars in the locality of 68°N and 233°E on 25 May 2008. Part of the science payload is the Magnetic Properties Experiments (MPE) that consists of two main experiments: the Improved Sweep Magnet Experiment (ISWEEP) and 10 sets of two Microscopy, Electrochemistry, and Conductivity Analyzer (MECA) magnet substrates with embedded permanent magnets of different strength. The ISWEEP experiment is, as the name indicates, an improved version of the Sweep Magnet Experiments flown onboard the two Mars Exploration Rovers (MERs) Spirit and Opportunity. The sweep magnet is ring shaped and is designed to allow only nonmagnetic particles to enter a small circular area at the center of the surface of this structure. Results from this experiment have shown that on the MERs hardly any particles can be detected in the central area of this ring-shaped magnet. From this we have concluded that essentially all particles in the Martian atmosphere are magnetic in the sense that they are attracted to permanent magnets. In order to improve the sensitivity of the Sweep Magnet Experiment for detection of nonmagnetic or very weakly magnetic particles, the ISWEEP holds six ring-shaped magnets, somewhat larger than the sweep magnet of the MERs, and with six different background colors in the central area. The six different colors provide new possibilities for improved contrast between these background colors, i.e., any putative nonmagnetic particles should render these more easily detectable. The Surface Stereo Imager will also take advantage of the small clean areas in the ISWEEPs and use the presumably constant colors for radiometric calibration of images. The MECA magnets work as substrates in the MECA microscopy experiments; they are built to attract and hold magnetic particles from dust samples. The collected dust will then be examined by the optical microscope and the atomic force microscope in the MECA package.

Citation: Leer, K., et al. (2008), Magnetic properties experiments and the Surface Stereo Imager calibration target onboard the Mars Phoenix 2007 Lander: Design, calibration, and science goals, *J. Geophys. Res.*, 113, E00A16, doi:10.1029/2007JE003014.

¹Niels Bohr Institute, University of Copenhagen, Copenhagen, Denmark.

²Department of Electrical and Electronic Engineering, Imperial College, London, UK.

³Institute of Microtechnology, University of Neuchâtel, Neuchâtel, Switzerland.

⁴Department of Atmospheric Science, Texas A&M University, College Station, Texas, USA.

⁵Jet Propulsion Laboratory, Caltech, Pasadena, California, USA.

⁶Max Planck Institut für Sonnensystemforschung, Lindau, Germany.

⁷SETI Institute, Mountain View, California, USA.

⁸Department of Physics, University of Central Florida, Orlando, Florida, USA.

⁹Lunar and Planetary Laboratory, University of Arizona, Tucson, Arizona, USA.

1. Introduction

[2] The main science objective of the Phoenix mission is to study the water ice deposit hidden in the underground in Martian arctic [Smith *et al.*, 2008]. Great amount of hydrogen was discovered by the Gamma Ray Spectrometer on Mars Odyssey [Boynton *et al.*, 2002; Mitrofanov *et al.*, 2002] and this hydrogen is believed to be bound in water. Phoenix will provide ground truth for these observations and will study the distribution of H₂O and CO₂ in subsurface layers. No mission to Mars has landed as far north as Phoenix and this will therefore be an opportunity to study also the dust in this region for comparison with results from previous missions. Dust is an important factor for the albedo properties of both ice and soil surfaces, will influ-

ence the mechanical properties of ice and thermal properties of the atmosphere and for these reasons properties of the dust is particularly interesting in the polar environment.

[3] The Improved Sweep Magnet Experiment (ISWEEP) onboard Phoenix will study if all particles in the Martian atmosphere really are magnetic as it was discovered by the Mars Exploration Rovers and the ISWEEPs will also work as a new kind of radiometric calibration target for the cameras on Phoenix.

[4] The magnet substrates in the Microscopy, Electrochemistry, and Conductivity Analyzer (MECA) a designed to (1) hold samples for analysis with the optical microscope and the atomic force microscope in MECA and (2) if possible estimate the saturation magnetization of the samples captured by the magnets.

[5] Even though none of the two experiments are exactly similar to previously flown magnetic properties experiments, the results will be used to compare with dust analyzed on other locations of Mars in order to understand if the properties of dust varies with latitude on Mars.

1.1. Magnetic Dust on Mars

[6] Since the Viking mission it has been known that the airborne Martian dust and the topsoil are magnetic in the sense that the particles are attracted to permanent magnets [Hargraves *et al.*, 1977, 1979]. The Mars Pathfinder mission in 1997 carried, along with a few other magnetic properties experiments, a magnet array with five magnets of different strength. On the basis of the results from this experiment it was estimated that the dust in the Martian atmosphere has an average saturation magnetization of about 2–4 A m²kg⁻¹ [Hviid *et al.*, 1997; Madsen *et al.*, 1999], which has later been extended to 1–4 A m²kg⁻¹ [Morris *et al.*, 2001; Gunnlaugsson, 2000]. These two missions also measured the elemental composition of selected targets on the landing sites by X-ray fluorescence spectroscopy. These measurements showed that the Fe content of soils and rocks is between 12 and 18% wt [Toulmin *et al.*, 1977; Rieder *et al.*, 1997]. However, it still remained to be clarified which iron oxide(s) carried the Fe, i.e., what was the mineralogical explanation for the dust being magnetic and what was the oxidation state of the iron.

[7] The MPEs on the two identical Mars Exploration Rovers, Spirit and Opportunity, [Squyres *et al.*, 2003; Madsen *et al.*, 2003; Gorevan *et al.*, 2003] had as the main science goal to identify the magnetic mineral responsible for the magnetization of the Martian dust and soils and if possible to reveal implications on the global influence of water on Mars.

[8] The composition of magnetic phases in the dust can help us understand how it was formed. The four most likely pathways are (1) volcanism, (2) meteor impacts, (3) interaction with liquid water, or (4) gas-solid interaction. For details on the different processes, see Madsen *et al.* [2003] and references therein.

[9] The two rovers are equipped with seven magnets each: The Capture magnet, the Filter magnet, the sweep magnet and four Rock Abrasion Tool (RAT) magnets. In this work only the three first are of direct interest and only these will be discussed.

1.2. Results From the Capture and the Filter Magnet on the MERs

[10] The Capture and Filter magnets are designed to collect dust from the atmosphere. The magnets are both made of Sm₂Co₁₇, which is built into an aluminum structure, though the design of the magnets is different: The Capture magnet is made as strong as possible to attract as much magnetic dust as possible, while the Filter magnet has a lower attracting force and therefore mainly attracts and holds the most magnetic of the airborne particles. The magnets are tilted 45° with respect to horizontal and positioned on the rover deck in front of the camera mast, just above the robotic arm, which is known as the Instrument Deployment Device (IDD). The tilt of the magnet surfaces helps removal of nonmagnetic and weaker magnetic material from the two magnets by wind or shaking during rover movement thereby further concentrating the magnetic phase in the dust. With this location of the magnets it is possible to investigate the collected dust with all three IDD instruments, i.e., the Mössbauer spectrometer, MIMOS II [Klingelhöfer *et al.*, 2003], the alpha particle X-ray spectrometer APXS [Rieder *et al.*, 2003] and the Microscopic Imager, MI [Herkenhoff *et al.*, 2003]. The two magnets are also placed just below the Panoramic Camera, Pancam [Bell *et al.*, 2003], which makes it possible to image the magnets and get visible and near-infrared spectra of the dust captured on the magnets. The combination of all these different kinds of measurements of the same sample has given the opportunity of the most detailed in situ examination of the dust in the Martian atmosphere to this date.

[11] Results from the Capture and Filter magnet experiments on the rovers show that, (1) magnetite (Fe₃O₄), possibly nonstoichiometric, is responsible for the magnetism in the dust; (2) nanophase oxides or oxyhydroxides and (likely) hematite (α -Fe₂O₃) are responsible for the yellowish/reddish color of the dust; and (3) olivine is present, even when wind events have removed the least magnetic dust particles. This shows that olivine is intimately associated with many of the dust particles and because olivine weathers relatively easily that liquid water cannot have played a major role in the formation of the dust [Goetz *et al.*, 2005].

[12] It should be noted here that pure, stoichiometric magnetite has a saturation magnetization $\sigma_s = 92$ A m²kg⁻¹, while pure hematite above the Morin transition temperature has $\sigma_s = 0.4$ A m²kg⁻¹. Therefore only few percent of magnetite is needed to account for the observed magnetization of the Martian dust and any additional hematite and oxyhydroxides will mainly contribute to the color of the dust with only little influence on its overall magnetization.

1.3. Results From the Sweep Magnet on the MERs

[13] The sweep magnet on the MERs is designed to detect and possibly identify nonmagnetic particles in the Martian atmosphere if such particles should be present. The sweep magnet is ring shaped, extremely strong and mounted only 0.4 mm below the aluminum surface. In this way only nonmagnetic or very weakly magnetic particles can settle in the center. The ring has an outer diameter of 9 mm, inner diameter of 4 mm and is 5 mm thick. It is made of Sm₂Co₁₇ and is built into an aluminum structure, which is somewhat larger than the magnet, leaving



Figure 1. Images of the sweep magnet on the Mars Exploration Rover Spirit. Images obtained at (left) sol 29, (middle) sol 400, and (right) sol 810, respectively. The magnet housing is 20 mm on the long axis and 14 mm on the short axis. The ring-shaped sweep magnet is 9 mm in outer diameter and revealed by the reddish dust.

the outer part virtually unaffected by the presence of the magnet (see Figure 1).

[14] The sweep magnet is placed very close to the radiometric calibration target for the Pancam and has therefore been imaged on almost every sol. Imaging with Pancam is the only possible way to examine the amount and distribution of dust on the sweep magnet. So far the analyses of the sweep magnet images show only few if any particles in the center of the magnet (*Bertelsen et al.* [2004], numerous abstracts, and M. B. Madsen et al. (Overview of the Magnetic Properties Experiments on the Mars Exploration Rovers, submitted to *Journal of Geophysical Research*, 2008)). This shows that the dust particles are essentially composite in nature and that each particle seems to contain probably at least a small amount of most if not all of the mineral components identified in the dust captured and held by the Capture and Filter magnets. Therefore, the result lends strong support to the idea that almost all particles in the Martian atmosphere contain at least a small amount of a strongly magnetic phase (magnetite), and as a result of this essentially all particles in the Martian atmosphere are more or less magnetic.

1.4. Perspectives

[15] It is surprising to find that essentially *all* dust in the Martian atmosphere should be magnetic. Can this really be true? Is this conclusion based on an experiment with too low sensitivity to really settle this question? One problem could be that dust settling in the center of the MER sweep magnets has a color too similar to that of the magnet's active surface (aluminum) and therefore remains undetected. Therefore a more sensitive experiment is desired.

[16] As discussed above, one result of the magnetic properties investigations that have been performed on previous missions is that all the airborne dust particles seem to be composite, i.e., to consist of some sort of agglomerate of crystallites of different minerals of which one or more are responsible for the magnetic properties of the particles. During the Phoenix mission optical microscope (OM) and atomic force microscope (AFM) images of Martian dust and soil particles will bring new knowledge on the detailed morphology of these particles and on their composite nature. Thereby the magnetic properties investigations may contribute to the knowledge about the history of water on the planet.

2. Description of the Magnetic Properties Experiments on Phoenix

[17] Each of the three ISWEEPs consists of six individual sweep magnet assemblies built into a black anodized

aluminum structure. The aluminum structure is 52 mm in diameter and the magnets have been increased somewhat in size compared to the sweep magnets on the MER Rovers: They have an outer diameter of 11 mm, an inner diameter of 5 mm and are 7 mm in height and (as for the rover sweep magnets) the magnetic material used for the magnets is $\text{Sm}_2\text{Co}_{17}$. At the surface of the instrument and at the symmetry axis of each magnet the magnetic field is 0.40 T and the field gradient is 440 Tm^{-1} by design. Calculated values were validated using a Hall probe.

2.1. Improved Sensitivity Sweep Magnet Experiment / SSI Calibration Targets

[18] In each of the sweep magnets a color chip is mounted (manufactured and provided by Dan Britt, University of Central Florida). The color chip has been prepared by suspending an inorganic pigment material in a GE RTV 655 silicone matrix. The pigments are chromium oxide (green), cobalt (blue), goethite (orange/brown) and three shades of gray made of different mixtures of TiO_2 and carbon black. These three shades of gray have reflectance values of approximately 20, 40, and 60%.

[19] The large color chips are shaped somewhat similar to a mushroom so their stem will fit into the bore of the cylindrical sweep magnets and cover the end face of the magnets with a flat, circular mat. In this way, the function of each sweep magnet will be similar to the MER sweep magnets, but with the silicone rubber providing surfaces with different background color for each magnet and thus (we believe) significantly improving the sensitivity for detection of nonmagnetic particles in the area in the center of the ring magnets (see Figure 2).



Figure 2. The ISWEEP magnet experiment and radiometric calibration target for the SSI. Six sweep magnets are built into an aluminum structure and covered with six different colors. The three small white spots are 0.75 mm in diameter and serves as internal fiducial points for the ISWEEP experiment. The black anodized housing is 52 mm in diameter.

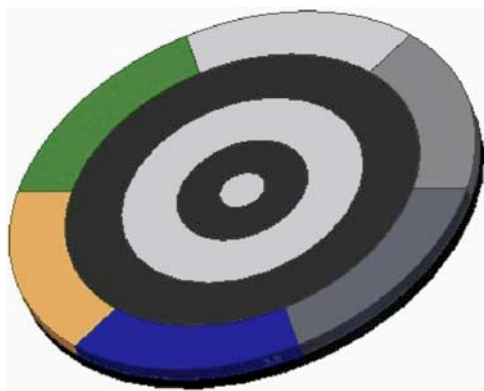


Figure 3. The SSI fiducial point targets work as orientation markers supporting the Robotic Arm operations and these targets also work as zero magnetic field color reference targets for the Magnetic Properties Experiment. The disk shown is 33.4 mm in diameter.

2.1.1. Color Dots in an Intermediate Strength Magnetic Field

[20] In the central part of the ISWEEP there are ten small color dots that are not directly protected by the fields of the magnets. Six of them have the same colors (and are made of the same material) as the color chips on the sweep magnets, the four others are experimental dots. These six will together with the central areas and rims of the mushroom shaped color chips provide information on the magnetization of the material attracted to the rims and dots (more on this later). Note that we distinguish between dots and chips: Dots are the small ones in the central part, while chips are the larger, mushroom shaped structures that cover the magnets. Three of the four experimental dots are pigmented RTV dots treated with thin layers of film of different metals: gold, copper, palladium and the last one is pure RTV. They serve as a test of an alternative way of keeping a small area clean of dust [Sabri *et al.*, 2008].

2.1.2. SSI Radiometric Calibration Targets

[21] Since the sweep magnets are intended to keep the central part of the color chips as clean of magnetic dust as possible, the ISWEEPs also have a second purpose: Namely to serve as radiometric calibration targets for the Surface Stereo Imager (SSI). The ISWEEP is therefore also referred to as the Radiometric Calibration Target (RCT) for the SSI or in short just cal target.

[22] There are altogether three ISWEEP magnets on the Phoenix Lander placed within the line of sight of the SSI in the deployed position.

[23] The individual ISWEEPs/RCTs have been given a serial number of the form NBI-Px-00xx, where NBI refers to the Niels Bohr Institute, Px to the Phoenix project and the last four digits is the individual number of each target. The targets chosen for flight are: NBI-Px-0025 (RCT1), NBI-Px-0022 (RCT2), and NBI-Px-0019 (RCT3). The ISWEEPs are placed at distances from the SSI almost half the distance to best focus. In the table below the position of the different ISWEEPs are given with respect to the SSI:

[24] The three ISWEEPs are placed on the Lander deck at widely varying azimuthal angle of the viewing direction of the SSI, making it always possible to find an ISWEEP under illumination conditions similar to the area on the surface for

which well calibrated images are desired (see the section on calibration).

2.1.3. Fiducial Point Targets as Zero Field References for MPE

[25] There are four SSI fiducial point (see Figure 3) targets on the Phoenix Lander of which three are provided by the Danish magnetic properties investigation team. The Danish supplied fiducial targets primarily work as orientation markers for the SSI to provide a well-calibrated reference for the in-flight development of a precise 3-D map of the work area of the robotic arm and the Lander deck, thus supporting the Robotic Arm operations.

[26] The fiducial targets are made of titanium. They are 33.4 mm in diameter and covered with the same type of colored RTV material as the color chips and dots in the ISWEEPs. The fiducials will therefore also be useful for the Magnetic Properties Experiments (MPE) since they will work as a zero magnetic field reference for dust sedimentation. These targets are placed on the Lander instrument deck in positions where they are not influenced by magnets in any way and the dust sedimentation rate in zero magnetic field can thus be measured by observing the amount of dust settling on the fiducial targets.

[27] The UV irradiation on the Martian surface can alter the optical properties of most reflecting materials. Therefore all color chips, dots and experimental dots have been artificially aged by exposure to UV irradiation corresponding to 2 months of exposure on the Martian surface, thus minimizing any further changes in the optical properties of the ISWEEPs during the primary mission.

2.2. Science Goals for the ISWEEP Experiment

[28] We will use the ISWEEPs and fiducials for an evaluation of the magnetic susceptibility of airborne dust by analysis of spectra recorded on areas on the ISWEEP structures and on the fiducial targets. This analysis will be based primarily on simulation experiments performed in a small dust sedimentation chamber in Copenhagen. The chamber works at Earth ambient pressure and temperature. Simulation experiments with dust derived from a number of minerals and natural mineralogical samples have been performed with versions of the ISWEEPs that are, in regard to magnetism, in all respects identical to the Phoenix flight units. However, in order to facilitate investigation of the interaction between the dust samples and the ISWEEP, particularly for spectroscopic analysis of the dust accumulated on different surfaces, the ISWEEP was equipped with light gray (60% reflectivity) color chips exclusively [Drube, 2006]. The conclusion of these validation and characterization experiments is that it is indeed possible to distinguish between three samples with substantially different saturation magnetization, i.e., pure goethite ($\sigma_s \sim 0.0 \text{ A m}^2\text{kg}^{-1}$), pure hematite ($\sigma_s = 0.4 \text{ A m}^2\text{kg}^{-1}$), and a thermally decomposed sample of the nontronite “Riverside” ($\sigma_s = 6 \text{ A m}^2\text{kg}^{-1}$). In short the purpose of the ISWEEPs is twofold (1) to determine if all particles in the Martian atmosphere are magnetic in the sense that they are attracted to permanent magnets or, if this is not the case, obtain as much information as possible about the nonmagnetic fraction of particles in the airborne dust and (2) to serve as a radiometric reflectance calibration target for the Surface Stereo Imager and for the Robotic Arm Camera.

Table 1. Placement of the Three ISWEEPs on the Phoenix Lander Relative to the SSI (Seen in the Payload Frame)

Phoenix Lander Deck	ISWEEP1/ RCT1	ISWEEP2/ RCT 2	ISWEEP3/ RCT3
Azimuth	-183.7°	-302.7°	-256.9°
Elevation	-47.1°	-31.3°	-30.8°
Distance	1052 mm	1502 mm	1592 mm
Placement	Close to LIDAR	Close to TEGA	Close to MECA
NBI serial number	NBI-Px-0025	NBI-Px-0022	NBI-Px-0019

2.3. Calibration of ISWEEPs

[29] Besides being a magnetic properties experiment, the ISWEEPs will also serve as radiometric calibration targets for the SSI in order to verify, validate, and maintain the SSI preflight calibration. Therefore each individual ISWEEP has been calibrated in great detail in the laboratory.

[30] The three ISWEEPs are placed in three different viewing positions with respect to the SSI (emission angles of 30.8, 31.3, and 47.2°, respectively) on the Phoenix Lander deck (see Table 1). Two of the ISWEEPs will exhibit very similar viewing angles (31.3 and 30.8°) as seen from the SSI, which for all practical purposes corresponds to an emission angle of 30° (the angle for which these targets were calibrated). Since it was not decided before calibration in which position each of the individual ISWEEPs should be placed on the Lander deck, all flight and flight spares were calibrated for both viewing angles (30 and 47°). Figure 4 shows the position of the ISWEEPs

on the Lander deck. One of the ISWEEPs (RCT 2) can also serve as a calibration target for the Robotic Arm Camera (RAC) [Keller et al., 2008].

2.3.1. Calibration Setup

[31] A facility has been set up for the calibration of the SSI radiometric calibration targets. It has not been possible to use a copy of the flight SSI for the complete calibration effort, but for the majority of the measurements an Avantes Avaspec 2048 spectrometer was used instead. The number 2048 refers to the number of pixels in the linear CCD detector. The spectrometer is not an imaging instrument and therefore operates much faster than the SSI, with better resolution and covering all relevant SSI wavelengths (445–1001 nm). The illumination used is an incandescent lamp with a continuous spectrum and a color temperature in the middle of the visible part of the spectrum. The measured quantity is the relative reflective power as function of wavelength. In addition measurements were made during ATLO using selected filters of the flight SSI and imaging all three calibration targets on the Lander instrument deck.

[32] On Mars light scattered by suspended atmospheric dust usually represents a substantial secondary source of illumination in addition to the direct sunlight. Since the amount of atmospheric dust and skylight varies significantly over time it is in practice impossible to take this contribution into account during calibration. Therefore only the direct almost parallel light from the light source has been used for the calibration. Some measurements of directional-hemispherical reflective properties of the color chips of the

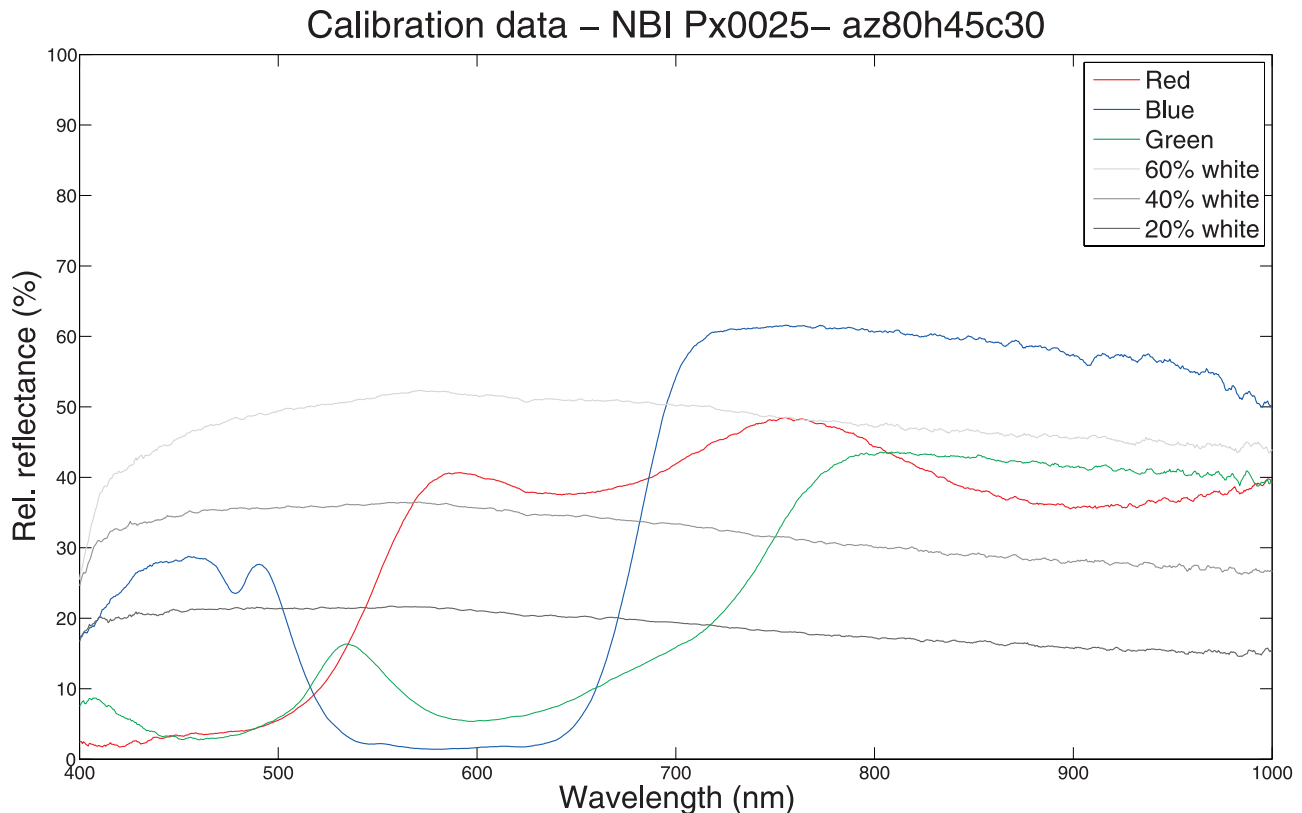


Figure 4. Reflectance spectra of the six color chips from the ISWEEP NBI-Px-0025. The light source is elevated 45° and has an azimuthal angle of 80° with respect to the ISWEEP, which is viewed from an emission (camera) angle of 30°.

Table 2. Selected Angle Settings in the Calibration Setup^a

Elevation Angle (4 Settings)	Emission Angle (2 Settings)	Azimuthal Angle (10 Settings)
15°, 30°, 45°, 60° 90°	30°, 47.2° 30°, 47.2°	~0°, 20°, 40°, . . . , 180° –

^aThe elevation angle and the emission angle are defined with respect to the surface so that 0° is in the plan of the ISWEEP and 90° is parallel to the normal. The azimuth angle is defined so that 0° is when the camera and the light source are pointed in the same direction.

calibration targets were performed as part of the validation and verification procedures of (flight spares) of the calibration targets.

[33] All calibration measurements are given as the relative reflectance, R , as a function of wavelength

$$R_n = \frac{\text{sample}_n - \text{dark}_n}{\text{white}_n - \text{dark}_n},$$

where n specifies the pixel number on the CCD detector, and the terms “white” and “dark” represent the data number obtained for the white reference target and absence of light, respectively. Since the reflectance is measured relative to the certified white reference, the spectral properties of the light source used during calibration of the targets are of less importance. The white reference target is made of Spectralon SRS-99 by Labsphere Inc. and reflects about 98% of all light in the visible and near-infrared spectral domain.

[34] The setup consists of two goniometers where it is possible to mount optical fibers connected to both the light source and the spectrometer. The incidence and emission angles are measured with respect to the plane where the target of interest is placed, so that 0° is in this plane and 90° is orthogonal to it. The elevation angle of the spectrometer is referred to as the viewing or emission angle, while the angle of the light source is referred to as the elevation angle. The angular position of light and detector (fiber) is better than one degree in both azimuth and elevation.

[35] The position of the light source is varied among five different elevation angles with respect to the surface plane of the color chips of the ISWEEP under investigation and 10 different azimuth angles for each of these elevation angles (measured so that 0° is when light and camera are in the same angle). All reflectivity data have been acquired for emission angles of both 30.5° and 47.2°, corresponding to the two different positions of ISWEEPs with respect to the SSI. The elevation angles of the light source cover the possible motion of the sun in the Martian sky including a possible tilt of the Phoenix Lander up to 12°, which is the maximum tolerance. This gives altogether 82 different lighting-viewing geometries (see details in Table 2). Finally, as part of the verification and characterization of the targets hemispherical-directional reflectivity has been measured for selected representative silicone rubber chips of some of the ISWEEPs.

2.3.2. Calibration of the Spectrometer

[36] The Avantes spectrometer has more than 20 well-defined reference spectral lines to calibrate the wavelength scale. In this setup a deuterium and halogen light source has been used to find the relation between the pixel number and the actual wavelength. The calibration was redone after a

few months and this showed that the spectrometer calibration is constant over time.

2.3.3. Results of Calibration

[37] Each of the three flight units and the flight spare ISWEEPs were carefully calibrated. Each of the six color chips on the sweep magnets, each of the four experimental dots and the black background color of the anodized aluminum were measured at both emission angles (30 and 47°) and for all 41 different angular positions of the light source. Below are shown typical spectra of the six color chips.

[38] It should be noted, that the three shades of gray do not have exactly the desired reflectivity of 20, 40, and 60% in all viewing positions. This small discrepancy is not of any importance since the ISWEEPs are calibrated and the exact reflectivity values are known. The accuracy of the absolute reflectivity is within $\pm 4\%$ in the range 445–900 nm and $\pm 8\%$ above 900 nm. The four experimental dots show low reflectivity for all wavelengths in most viewing angles. This is a consequence of a very strong specular component in their reflectivity. Figure 5 give a typical example of how they behave at an azimuth angle where specular reflection is absent in the emission direction, here for an azimuthal angle of 80°.

[39] Note that the anodized aluminum is black in the visible part of the spectrum, but has a significant reflectivity in the near infrared part of the spectrum. When the light source was almost in the specular position with respect to the detector of the spectrometer (i.e., the azimuth angle was 160 or 180°) the spectra were very noisy and of bad quality, simply because of a very strong specular reflection of the experimental dots. When using the ISWEEPs for calibration of SSI images, it is therefore necessary to use an ISWEEP where the azimuth angle between the incident light from the sun and the emitted light from the ISWEEP as seen by the SSI is less than 140°. Since the azimuth angle between the two ISWEEPs with greatest separation is almost 120° it will always be possible to find an ISWEEP that fulfills this requirement.

2.3.4. Evaluation of Calibration Data

[40] Since the ISWEEPs also work as radiometric calibration targets for the SSI, the calibration data for the three flight ISWEEPs and the flight spare target has been subject to an intensive study. The calibration data of these four targets has been compared to two other targets that have been built for comparative studies and as spare targets (Ids NBI-Px-0014 and NBI-Px-0021). The data for the six ISWEEPs were expected to be identical, as both the color chips and the supporting structure were produced from the same batch of material under identical conditions. However, the calibration data were not perfectly consistent. The spectral shape was preserved, but the intensity seemed to vary from one ISWEEP to another. The spectral data for ISWEEPs 0014, 0021, and 0022 were virtually indistinguishable. The experimental setup described in section 2.3.1 is rather sensitive as the angles in the setup are easily compromised. Altering angles also alters the intensity of the spectra viewed, leaving the spectral shape intact, so this could very well be the explanation for the slightly differing data sets. Another explanation can be that the ISWEEPs are indeed different; mainly the local curvature can vary and thereby give minor changes in the spectra. It would actually be surprising if they were perfectly identical.

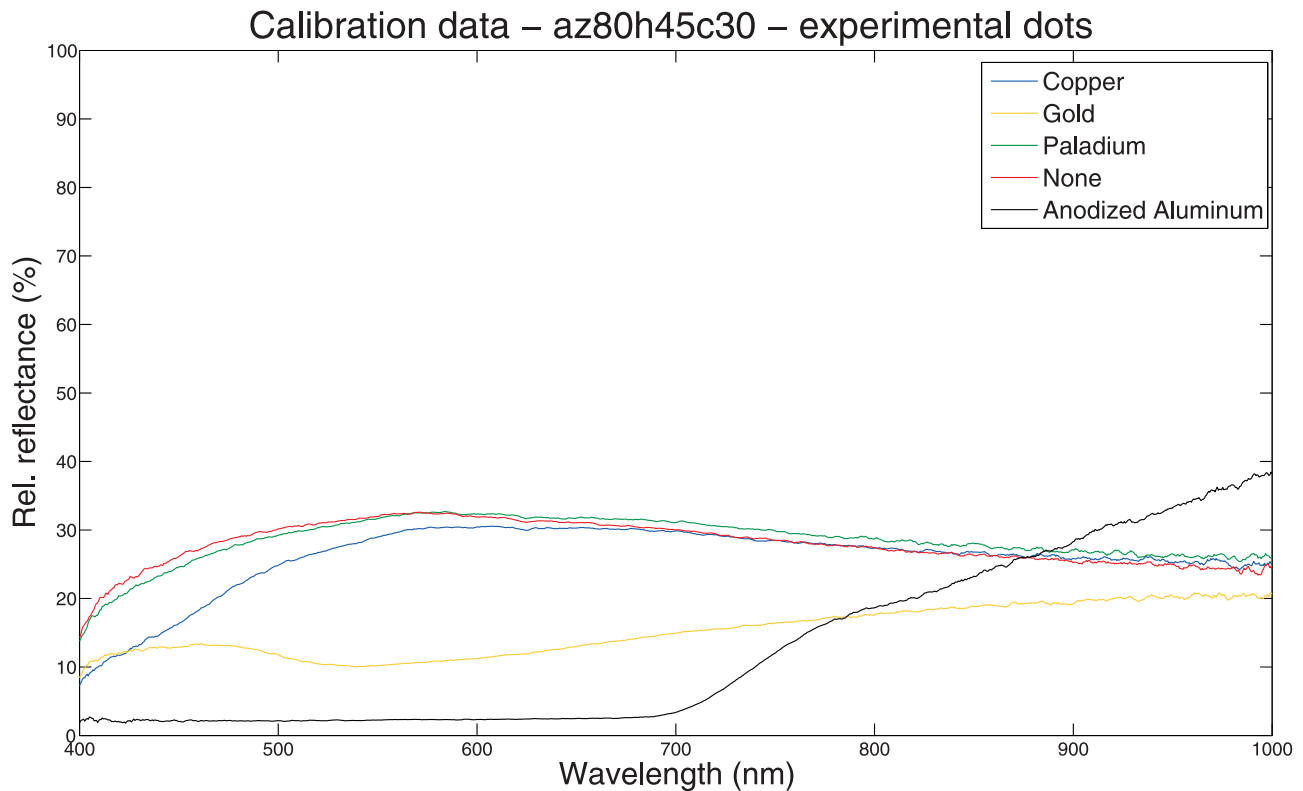


Figure 5. Reflectance spectra of the experimental dots and of the black anodized aluminum structure, which the magnets are built into.

[41] ISWEEPs 0014 and 0021 were tested and calibrated under very controlled conditions, with ample time to repeat the experiments etc., so this data must be assumed to be of a quality at least equal to the data generated for the three flight units and the flight spare. Therefore one possible strategy for flight calibration would be to calibrate all the ISWEEPs to an average spectrum of ISWEEPs 0014, 0021, and 0022 for the viewing angles 29.4 and 31.3°, and to use an average of the calibration results from the ISWEEPs 0014 and 0021 for the viewing angle 47.2°. Each combination of elevation and azimuth angle will require its own calibration spectrum.

[42] For bidirectional calibration the chips are sampled in the way that our calibration setup with its optical waveguides “sees” only a small fraction (“the detection area”) of the surface of each color chip. The dependence of placement of the detection area on the color chip was also investigated, and the result of this investigation was that only the blue color chip was sensitive to this placement. It has not been possible to finally determine if the differences in the calibration data are due to actual difference in the ISWEEPs or can be explained by uncertainty in the measurements.

[43] The ISWEEP 0022 (RCT 2) is not only the ISWEEP with the highest consistency in terms of spectral data, but it is also the primary ISWEEP to be used for calibration of the SSI. For the blue color chip caution is advised when using this color for calibration purposes.

2.4. MECA Magnet Substrates

[44] The MECA (Microscopy, Electrochemistry and Conductivity Analyzer) [Hecht et al., 2008] consists of a

microscopy station with an optical microscope (OM, resolution at target $\sim 4 \mu\text{m}$), and an atomic force microscope (AFM) with 8 disposable tips; a wet chemistry electrochemistry laboratory, where samples delivered by the robotic arm will each be dissolved in one of four beakers to determine pH, conductivity, salt content, and other electrochemical properties [Kounaves et al., 2008]; and the Thermal and Electrical Conductivity Probe (TECP) (A. Zent et al., The Thermal Electrical Conductivity Probe (TECP) for Phoenix, submitted to *Journal of Geophysical Research*, 2008) that is inserted into the ground by the robotic arm to measure subsurface thermal and electrical properties as well as humidity.

[45] Parts of the samples delivered by the RA will be brought to a combined sample wheel translational stage (SWTS), where a 200 μm slit rejects the larger particles. On the SWTS the samples will be collected by a subset of the 69 substrates that have different adhesion abilities. The substrates are arranged in sets of six, each with one sticky silicone substrate, one silicon substrate with a micromachined texture designed to hold micron-sized particles, two magnetic substrates, and two small “buckets” designed to hold bulk samples. The two magnet substrates have different magnetic field strength and hence different attractive forces and different abilities to attract and hold magnetic particles onto their surface. There are 10 such sets of substrates for investigation and comparison of a corresponding number of samples. These samples are either delivered by the robotic arm from different depths below the surface or acquired by so-called air fall experiments, where a set of substrates are exposed to the Martian atmosphere

Surface scans

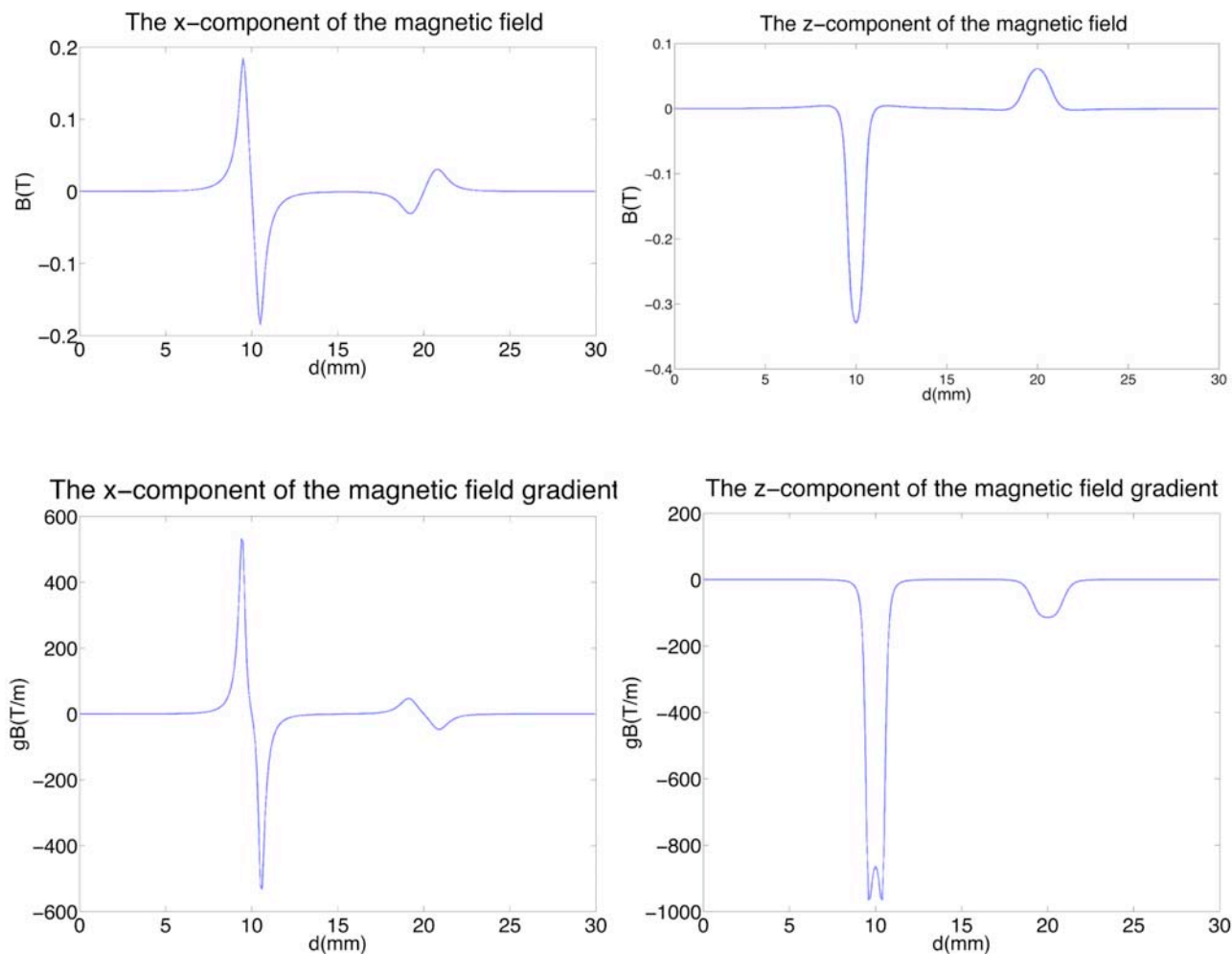


Figure 6. The plots show how the magnetic field and the magnetic field gradient change (left) along and (right) perpendicular to the scanning axis across the magnets. Note that in this diagram the distance between the two is 10 mm, the same distance as between weak and strong magnets on adjacent sets. Within a set of substrates in the SWTS, the MECA magnets are 19.88 mm apart.

and thereby collecting dust settling out of the atmosphere. Besides the ten sets of substrates there are nine calibration substrates, including also a tip-breaking device.

[46] Both OM and AFM will investigate the material attracted and held by the substrates, which will give the most detailed images of Martian dust to date. It will thus be possible to study shapes and sizes of very small particles giving new details on the origin of the Martian dust [Hecht *et al.*, 2008].

2.4.1. Design of MECA Magnet Substrates

[47] The two magnet substrates are built into almost identical housing structures. The only visible difference is the size of the holes where the magnets are placed. The housings are 4.05 mm in diameter (of which 3 mm is exposed by the SWTS) and 2.15 mm in height.

[48] The strong magnet is cylindrical, 1.8 mm thick and 1.0 mm in diameter. The weak magnet is also cylindrical and 0.3 mm thick and 1.6 mm in diameter. Figures 6 and 7

show the magnetic field and the magnetic field gradient from the two magnets. Two kinds of views of the magnetic field are displayed in Figures 6 and 7. Surface scans show how the magnetic field and the magnetic field gradient vary when moving across the surface of the magnets. The x- and y-axes are in the surface plane of the magnet structure, with the x-axis parallel to the scan direction. The z-direction is normal to the plane of the magnets. In these scans the y-components are zero and therefore not displayed. The other scan (along the z-axis) shows how the magnetic field and the magnetic field gradient vary in the z-direction with distance to the surface at the central symmetry axis of the magnet Figure 8.

2.4.2. Science Goals for the MECA Magnet Experiment

[49] The purpose of the microscopy station is to study size distributions and shapes of the smallest mineral grains on Mars, both sampled from the soil and from the atmo-

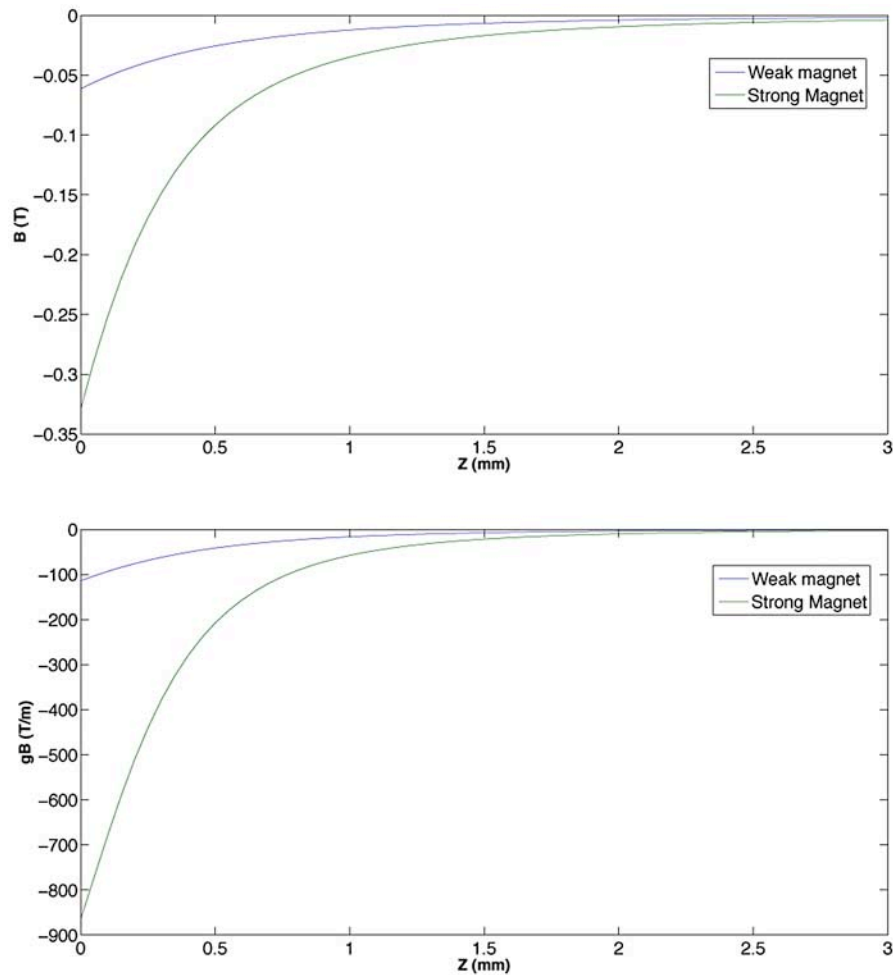


Figure 7. The z -component of the (top) magnetic field and (bottom) magnetic field gradient as a function of distance from the center of the magnets. Note that the two other components are 0.

sphere, in order to understand their origin and attempt to determine if water was present when they were formed and developed. The MECA magnets will work as substrates holding the samples for investigation by AFM and OM. For details see *Hecht et al.* [2008]. Furthermore the MECA magnets will be used to estimate the saturation magnetization of the particle samples held by the substrates.

2.5. Microscopy Simulation Experiments

[50] As preparation for the Phoenix operations, a series of microscopy simulation experiments has been made with the MECA magnets. The purpose of the simulation experiments was to understand what kind of measurement could be made of the dust collected by the magnets. This includes studies by the OM and by the AFM. It was considered of particular importance to investigate if it would be safe to make AFM scans of the dust on the magnets.

[51] The experiments were performed at the testbed at Imperial College in London. This testbed has an exact copy of the AFM scanner and the SWTS, whereas the optical microscope is slightly different from the OM in the MECA package. The testbed microscope has the same optics and the same light-emitting diode (LED) assembly as the

MECA OM, but uses a larger CCD (1600×1200 rather than 512×256 pixels). The setup is placed in a chamber that can be evacuated to Martian pressure, and eventually repressurized with nitrogen. In this work the pressure was about 1–5 mbar. Furthermore the chamber can be cooled to about -50°C , but in this work it was kept at room temperature. The testbed is equipped with a small scoop that can contain about 1 cm^3 of sample material and deliver it to a set of substrates similar to the scoop on the Robotic Arm. A series of simulation experiments have been performed, involving both (active) sample delivery by the scoop and (passive) dust settling from above.

2.5.1. Air Fall Experiments

[52] To simulate air fall experiments the dust sedimentation chamber at University of Copenhagen was used. The dust sedimentation chamber is a $70 \times 70 \times 135 \text{ cm}$ box, where magnets are placed on a shelf at the bottom and the dust samples can be blown in at the top and subsequently attracted by the magnets. The dust samples will be dispersed in the air in the chamber and can afterward fall and sediment out onto the magnets at atmospheric pressure and at room temperature.

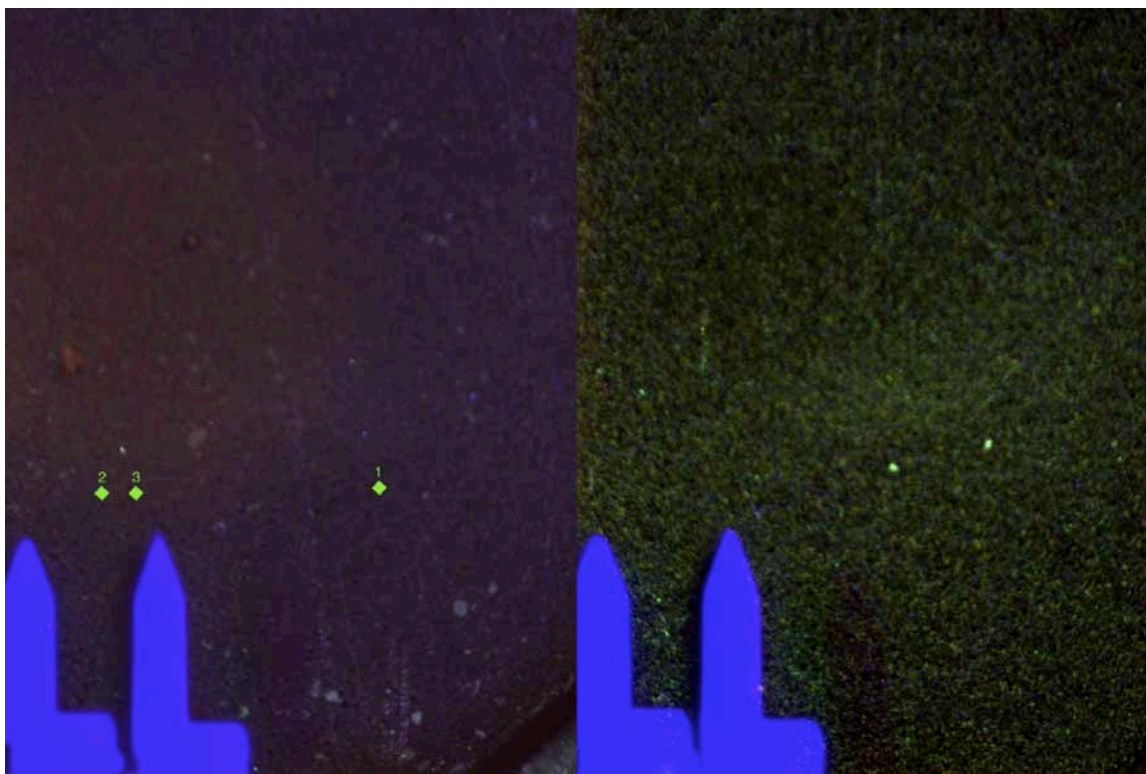


Figure 8. OM images of the (left) strong magnet and (right) weak magnet. The dust (Salten Skov) on the magnets is collected in an air fall experiment. The two blue features in the bottom are the AFM tips. These images are not true color. The green markers are locations chosen for AFM scans (see section 2.6).

[53] The particle size distribution in suspension in the air can be somewhat controlled by initially protecting the magnets against exposure of the airborne dust and introducing a known time period before such exposure is allowed. In this way the biggest particles are prevented from settling onto the magnets. For details on the dust sedimentation chamber, see *Drube* [2006].

2.5.2. Samples Used for Simulation Experiments

[54] In this work the following three different samples have been used to simulate sample acquisition by MECA substrates on Mars:

[55] 1. Salten Skov is dehydrated soil from the forest Salten, close to Aarhus, Denmark, and has magnetic properties somewhat similar to the Martian dust. The sample contains the iron minerals hematite, maghemite and goethite and various nonferrous silicates. The sample has an average saturation magnetization of $3.5 \text{ A m}^2\text{kg}^{-1}$ caused by the presence of maghemite in the sample. For details on the Salten Skov sample, see *Nornberg et al.* [2004] and *Bertelsen* [2001].

[56] 2. Pyrrhotite from Gossan Howard, Virginia. This sample is less magnetic than the Salten Skov soil with an average saturation magnetization of $1.0 \text{ A m}^2\text{kg}^{-1}$. Pyrrhotite is also chosen because this mineral has been found in some of the Shergottites (subgroup of meteorites from Mars) [*Rochette et al.*, 2001].

[57] 3. Allard Lake from Quebec in Canada is a rock that contains hemoilmenite. The mixture of ilmenite and hema-

tite gives a strong remnant magnetization, with average saturation magnetization of $0.5 \text{ A m}^2\text{kg}^{-1}$ [*Kletetschka et al.*, 2002; *Hargraves*, 1959].

[58] As mentioned in section 1.1 the Martian dust has an average saturation magnetization of $1\text{--}4 \text{ A m}^2\text{kg}^{-1}$, the average being probably closest to the low end of this range. Therefore these samples represent the range expected for the soil and dust on the Phoenix landing site.

2.6. OM Simulation Experiments

[59] Substrates prepared with the samples described above were studied using flight simulation experiments as follows.

2.6.1. Optical Microscopy on MECA Magnet Substrates: Air Fall Experiment

[60] A set of MECA magnets were exposed to air falling Salten Skov sample as described in 2.5.1. As a first approach to investigate the sample collected by the substrates, the substrates were examined by the OM. This gave an idea about the amount of material collected and was used to find good places to make AFM scans. To image the whole magnet, it was necessary to make three images, referred to as left, center and right image, respectively. Images were always recorded in sets of 3 with one of 3 colors of LEDs turned on making it possible from the acquired images to merge to RGB color images.

[61] Two AFM tips are visible in the OM images, since only one tip has been used. One of the blue LEDs is placed so that it is exactly in a specular reflecting angle with respect to the tips. Therefore the tips appear very blue in

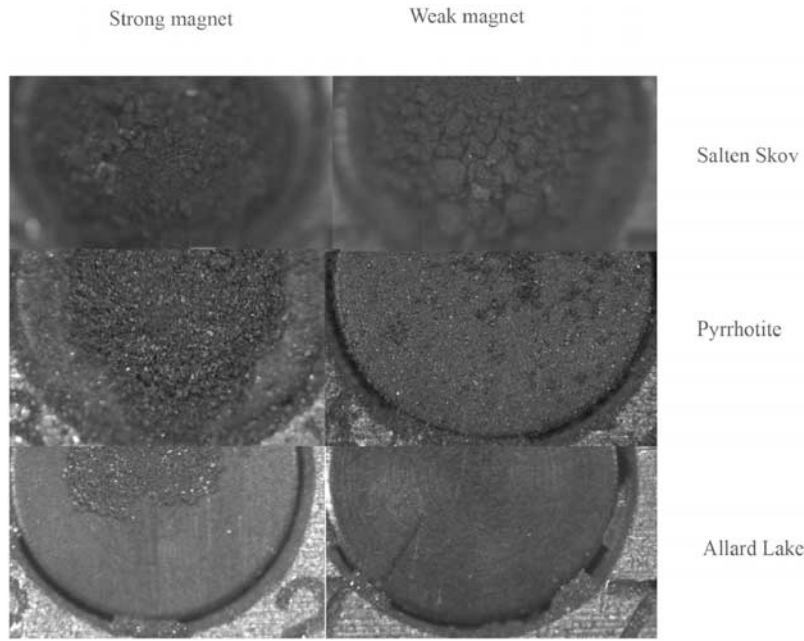


Figure 9. Three samples with different saturation magnetization collected by the MECA magnets. On the strong magnets the dust piles are about 720, 240, and 80 microns high for Salten Skov, Pyrrhotite, and Allard Lake, respectively. On the weak magnets there is only a real pile for the Salten Skov sample, while the other two samples only collect very little or no dust at all. Images are taken with blue LED on.

some of the following images and in general making the images appear blue when the three images are weighted equally in the color composite. All color OM images in the following are composed in the freeware program ImageJ and adjusted to some degree. The images are therefore not true color and cannot be directly compared. Within the time frame available it has not yet been possible to make perfect color calibration.

[62] Below images of the two magnets (strong and weak) exposed to air falling dust are shown. On these images it is difficult to see any dust on the weak magnet, but on the strong magnet there is lots of dust. Also big particles can be seen, which must be relatively magnetic since the surfaces of the magnets are in almost vertical position. The green markers show where AFM scans were made (see section 2.7).

2.6.2. Optical Microscopy on MECA Magnet Substrates: Scoop Delivery

[63] All three samples described in 2.5.2 were each dumped on three different sets of MECA magnets in order to study how samples with different saturation magnetization are collected by the magnets. Figure 9 shows the images obtained with the blue LED on.

[64] Note that the images are taken at different focus steps, giving an idea about the height of the pile of dust on the magnets. The OM can move in steps of 80 microns. In focus position 0 a clean substrate will be in focus.

[65] For the Salten Skov sample the image of the weak magnet is recorded with the OM in focus position 9, which means that the height of the sample pile is about 720 μm . The image of the strong magnet is recorded in focus position 8, which means that the pile is about 640 μm high. These piles are significantly higher than the 200 μm width of the slit at the opening of the SWTS, which shows either

that the magnets are attracting surplus material, when the wheel is rotating inside the MECA (or maybe less probable) that the magnetic particles attracted onto the magnet spontaneously form chains of these particles, chains that stand out from the surface of the magnet like hairs on a brush. Since the Salten Skov sample is believed to be slightly more magnetic on the average than the Martian soil, the observed heights on the magnets will probably be an upper limit for the amount of dust one can expect when the MECA is operating on Mars. It is surprising that the weak magnet collects more dust than the strong magnet. This can be explained by the rotation direction of the SWTS: The weak magnet is the first substrate in the rotation direction, meaning that all surplus material from the other substrates tumble over the weak magnet. The strong magnet is the last substrate in the rotation direction, and this means that a minimum of material passes by this substrate.

[66] For the Pyrrhotite sample the strong magnet is imaged in focus position 3 meaning that the pile is about 240 microns high. On the weak magnet small clusters of dust are found, showing that Pyrrhotite is probably about the least magnetic substance that can be held by the weak magnet.

[67] Allard Lake particles can only be collected by the strong magnet and only in a thin layer close to the central part of the magnet. The image of the strong magnet is in focus position 0.

[68] These three sets of images show that the amount of dust collected on the two kinds of magnets depends strongly on the saturation magnetization of the sample delivered. Therefore images obtained by the OM can be used to estimate the saturation magnetization of samples collected on Mars by comparing with Earth analog experiments. On

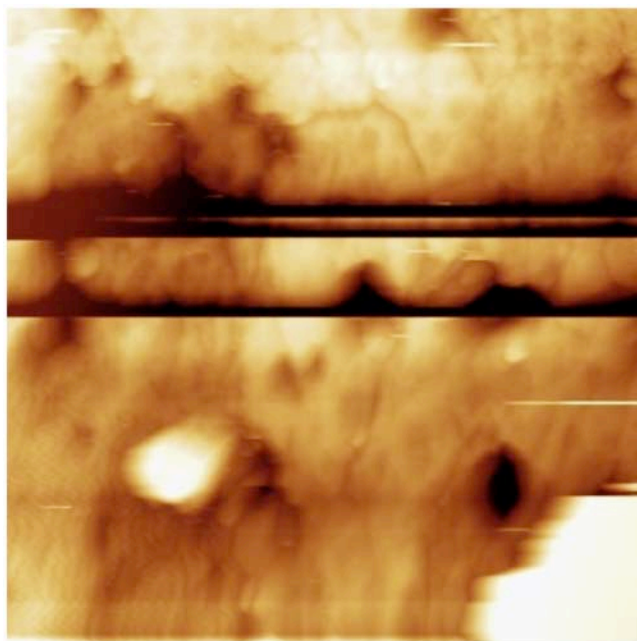


Figure 10. A $40 \times 40 \mu\text{m}$ AFM scan of location 2, showing a particle and holes from the anodizing and black lines, which may have been caused by smaller particles dragged along the surface by the tip.

Mars the gravitation is smaller, therefore a sample with a given saturation magnetization would result in a slightly larger dust pile on the magnet substrates on Mars. This means that the experiments as shown here can be used to estimate the upper limit for the saturation magnetization of the Martian soil.

2.7. AFM Simulation Experiments

[69] In the following, results of AFM scans will be shown. All scans are made as amplitude modulated AFM, a dynamic mode also known as tapping mode. For details on the AFM modes and the differences between them, see for instance *Garcia and Perez* [2002]. The OM images from the dump test, showed very large piles of dust. This may not be ideal for AFM scanning, since the dust is more likely to be pushed around by the tip.

[70] The OM images from the air fall experiment show on the other hand a relatively thin layer of dust on both magnets. The layer on the weak magnet is so thin that only very few particles can be found in the scanning area of the AFM. Therefore the strong magnet was chosen as target for AFM scanning. Three locations were selected (see Figure 8). Location 1 was chosen because the dust layer seemed to be so thin that the particles probably were not stacked in more than one layer. But the AFM scan did not show any particles at all; therefore the more densely populated location 2 was selected for a $40 \times 40 \mu\text{m}$ scan (the largest scanning area possible with this instrument, see Figure 10).

[71] Many interesting features can be seen on this scan. The black lines seen in the upper part of the image are probably caused by small particles that stick to the AFM tip. In the lower right corner a large white (high) area is observed. This is simply the limitation of the instrument,

which can create these features when operated at its full range ($40 \times 40 \mu\text{m}$). Next to the white area is a hole, about $10 \mu\text{m}$ deep; this type of hole is a result of the anodization process of the structural aluminum of the magnet substrate. The precise depth of the hole cannot be measured using the AFM since the cantilever hits the rim of the hole before the tip gets into contact with the bottom of the hole.

[72] In the lower left of the scan a high structure, believed to be a particle, is observed. The particle is about $4 \times 6 \mu\text{m}$ in diameter and $3.5 \mu\text{m}$ higher than the surroundings, thus it is a relatively spherical particle. The scan shows that it is possible to hold particles on the magnets and produce a useful scanning image with the AFM. As mentioned the black line can be caused by small particles that stick to the tip. In order to reproduce the experiment another area, location 3, was also scanned (see Figure 11).

[73] This scan is $12.7 \times 12.2 \mu\text{m}$. In the upper part of the image a small cluster of particles is seen. The particles are $2-3 \mu\text{m}$ in diameter and between 0.5 and $1.0 \mu\text{m}$ in height. These particles therefore appear more flat than the particle in location 2.

[74] The aim of this paper is not to make detailed analyzes and interpretation of the AFM scans and OM images, but rather to understand what kind of experiments can be made on the magnet substrates. The OM images show piles of about $700 \mu\text{m}$ in height on the magnets when samples are dumped by the scoop. Much of the material on the magnets in these cases is believed to be scavenged from the vicinity of the magnets when the SWTS is rotated inside the MECA after dumping. It is not considered to be safe to make AFM scans of these large piles of particles, eventually one can consider to scan the surface of single large particles. Dust collected by the magnets in air fall experiments were shown to be suitable for AFM scans and single particles

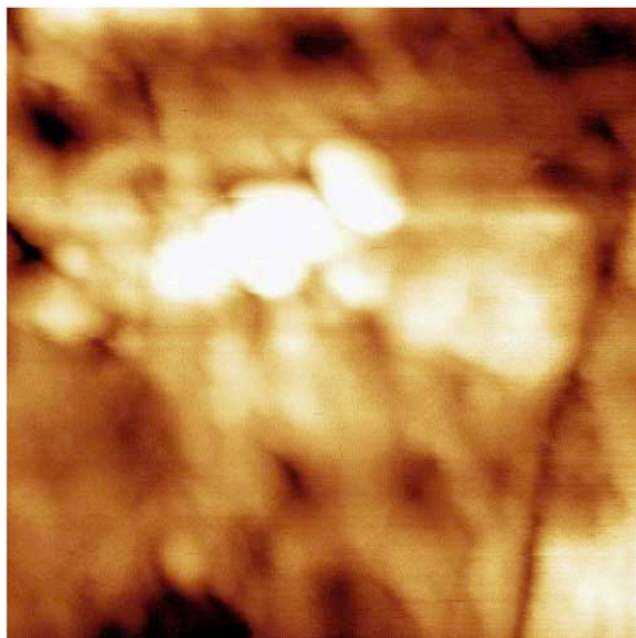


Figure 11. A $12.7 \times 12.2 \mu\text{m}$ AFM scan of location 3, showing particles $2-3 \mu\text{m}$ in diameter.

were detected. Sizes and morphologies of these particles can be determined.

3. Operations and Data Products

3.1. ISWEEP Operations

[75] All three ISWEEPs will serve as radiometric calibration targets for the SSI during landed operations and one of them (RCT 2, see Table 1) will also serve as a calibration target for the Robotic Arm Camera. Therefore the ISWEEPs will be periodically imaged whenever the SSI and the RAC are operating. The RCT 2 will be used as calibration target for the RAC and because this target is the one closest to the work area of the robotic arm, this target will probably also be one that is used the most when calibrating the SSI. With the expected level of imaging of the work area it should therefore be possible to monitor the dust collection on RCT 2 on a daily basis.

[76] The other two ISWEEPs will be imaged for radiometric calibration of panoramas, for spots of interest for mineralogical investigations. Using three calibration targets at widely different azimuthal angles makes it possible to better match the illumination conditions of the surroundings. Furthermore the RCT 1 and RCT 3 will also be imaged for scientific purposes as part of the magnetic properties investigation in order to study the dust sedimentation rate and to determine if any particles suspended in the atmosphere will be able to avoid the deflective power of the strong ring magnets of the ISWEEPs and thereby can settle in the centers of the 6 ring magnets of each ISWEEP.

3.1.1. Image Quality

[77] The majority of the 12-bits images recorded by the SSI will probably be returned either significantly compressed or losslessly compressed depending on the stage of the mission and of the scientific context in which they were recorded. Since imaging using the SSI (and in some cases the RAC) is the only way to study the dust collecting on the ISWEEPs and the associated fiducial targets it will be desirable to ensure the highest possible quality of these images. Even though the ISWEEPs are positioned relatively close to the SSI (1–1.6 m distance), they will still be so small in the images that it will be possible to significantly subframe the images of the ISWEEPs. Because the images will be used for calibration of other images the ISWEEP images will often make use of many filters. The central part of each magnet, which will be expected to be relatively clean of magnetic particles, will be at least 9 pixels across in an image. Also, because of their proximity to the SSI to have the best possible focus it will be desirable regularly to obtain images through the diopter lenses of the SSI.

3.1.2. Image Analysis for Interpretation of Magnetic Properties Experiment

[78] To provide a data set that will enable us to extract information about the magnetic properties of the airborne dust it will be important to periodically acquire high-resolution images in the full spectral range of both the ISWEEPs and of the fiducial targets. Also imaging of the same objects after strong wind gusts will provide important information, both about the magnetic properties of the dust and about possible separability into different subpopulations of dust and about the action of wind gusts. On the MERs changes in dust patterns have been regularly observed as

results of wind activity [Bertelsen *et al.*, 2004; M. B. Madsen *et al.*, submitted manuscript, 2008].

3.1.3. MECA Magnet Substrates Operations

[79] The magnet substrates are a part of the optical microscopy MECA experiments. The ten sets of MECA substrates will collect samples in two different ways: Either by air fall experiments (see 2.6) or by delivery of sampled material from the surface and subsurface by the scoop on the robotic arm. In both cases the substrates will be examined by the OM, and if suitable targets are identified, subsequently by the AFM. Shortly after landing an air fall experiment is planned.

3.1.4. MECA OM Data Products

[80] The OM is equipped with three LEDs (red, green, and blue) for illumination of the substrates of the SWTS during acquisition of images and an UV-emitting LED included for studies of fluorescent materials. The LEDs may be used in five different configurations; RGB, R, G, B, or UV individually, and “none.” Color images and spectral information can thus be extracted from the data products. Images are recorded on a 512×256 frame transfer CCD with 12 bits/pixel giving 0–4095 data numbers per pixel. For some substrates one image will cover a representative area, while for other substrates more than one image may be needed. For the magnetic substrates it is desired to acquire one or two images covering an area extending from the center of the substrate to the perimeter. For studies of the gravitational influence on grains held on the substrates it may be desirable to include both the top and bottom part of the perimeter for evaluation of all the forces acting on the particles. The resolution is about $8.8 \mu\text{m}$.

4. Conclusions

[81] The two magnetic properties experiments onboard the Phoenix Lander can give new insight to the formation and history of the dust on Mars. The six different background colors in each of the sweep magnets in the ISWEEPs significantly improves the possibility to detect any nonmagnetic or very weakly magnetic particles settling in the center compared to the Sweep Magnet Experiment on the Mars Exploration Rovers.

[82] Four fiducial targets are placed on the Lander deck. Three of the fiducial targets are made using the same pigmented silicone rubber as used on the ISWEEP and they will work as color reference for the ISWEEP experiment. Since the fiducial targets are positioned far away from any magnets, they will be used to measure the settling rate of dust in areas not influenced by magnetic forces.

[83] The combination of the ISWEEPs and the fiducial targets provides an opportunity to study other aspects of the magnetic properties of Martian atmospheric dust particles than have been possible before and will hopefully answer the questions with higher sensitivity that arose from the results of the Sweep Magnet Experiment on the Mars Exploration Rovers: Are all particles in the Martian atmosphere really magnetic and thereby composites of both magnetic and nonmagnetic material?

[84] Because of their surprising ability to stay comparatively clean of magnetic dust, the central part of each sweep magnet in the ISWEEPs will also be used as radiometric calibration target for the two cameras onboard the Phoenix

Lander: the Surface Stereo Imager (SSI) and the Robotic Arm Camera (RAC). Magnet substrates for the MECA microscopy station are like the other substrates designed to collect and hold samples either delivered by the scoop on the Robotic Arm or accumulated in air fall experiments. The samples on the MECA substrates can be examined by an optical microscope (OM) and by an atomic force microscope (AFM). Simulation experiments have shown that samples dumped by the scoop may result in piles on the magnet substrates several hundreds of microns high. Such large sample piles may not be suitable for AFM scans since the presence of many loosely bound particles may result in particles sticking to the AFM tip and disrupting the image (and contaminating the AFM tip for later use). On the other hand these large collections of sample are very good for optical microscope studies and the amount of dust collected by the magnets will be used to estimate the saturation magnetization of the samples delivered to MECA. Simulation experiments show that samples with different saturation magnetization settle differently on the two types of MECA magnets.

[85] In air fall simulation experiments the magnets have proven very good at attracting and holding material. The thin layer of relatively small particles that is expected to cover the magnet substrates after exposure to the Martian atmosphere is likely to be very suitable for AFM study. In simulation experiments several AFM images of particles were obtained from air fall simulation magnet substrates. OM and AFM images of Martian dust and soil particles will bring new knowledge on the morphology of these particles and thereby shed new light on the history of water on the planet.

[86] **Acknowledgments.** We would like to thank all those people who made this work possible, including Michael Bernt, Morten L. Christensen, Jørgen Jørgensen, and Per Thor Jonassen from the workshop at Niels Bohr Institute for invaluable contributions to both design and manufacture of the Danish equipment for Phoenix and the related tools and Tue Hassenkam, Nano-Science Center, University of Copenhagen and Noemi Rozlosnik, The Polymer Department, Risø National Laboratory, DTU for help with AFM simulation experiments. The results from this work have not been evaluated here, but it turned out to be a very fruitful pre-study, which was very valuable for this work. Also thanks go to Jaqueline Kløvgaard Jensen, Faculty of Life Sciences, University of Copenhagen; Mads Dam Ellehøj, Ice and Climate and Earth and Planetary Physics, Niels Bohr Institute, University of Copenhagen; and Michael Torben Hallundbæk and N. Zahles Gymnasieskole, Copenhagen and Andreas Lemark, Ice and Climate, Niels Bohr Institute, University of Copenhagen for all the work they put into the calibration of the Phoenix radiometric calibration targets. And finally thanks to the Danish Research Agency, the Lundbeck Foundation and Oticor for financial support and B. Hapke and an anonymous reviewer for their very constructive reviews that significantly improved this paper.

References

- Bell, J. F., III, et al. (2003), Mars Exploration Rover Athena Panoramic Camera (Pancam) investigation, *J. Geophys. Res.*, *108*(E12), 8063, doi:10.1029/2003JE002070.
- Bertelsen, P. (2001), Backscattering Mössbauer spectroscopy of magnetic dust on Mars, Ph.D. thesis, Niels Bohr Inst., Univ. of Copenhagen, Copenhagen.
- Bertelsen, P., et al. (2004), Magnetic Properties Experiments on the Mars Exploration Rover Spirit at Gusev Crater, *Science*, *305*, 827–829, doi:10.1126/science.1100112.
- Boynton, W. V., et al. (2002), Distribution of hydrogen in the near surface of Mars: Evidence of subsurface ice deposits, *Science*, *297*, 81–85, doi:10.1126/science.1073722.
- Drube, L. (2006), Simulation of dust sedimentation, M.S. thesis, Univ. of Copenhagen, Copenhagen.
- Garcia, R., and R. Perez (2002), Dynamic atomic force microscopy methods, *Surf. Sci. Rep.*, *47*, 197–301, doi:10.1016/S0167-5729(02)00077-8.
- Goetz, W., et al. (2005), Indication of drier periods on Mars from the chemistry and mineralogy of the atmospheric dust, *Nature*, *436*, 62–65, doi:10.1038/nature03807.
- Gorevan, S., et al. (2003), Rock Abrasion Tool: Mars Exploration Rover Mission, *J. Geophys. Res.*, *108*(E12), 8068, doi:10.1029/2003JE002061.
- Gunnlaugsson, H. P. (2000), Analysis of the magnetic properties experiment data from Mars: Results from Mars Pathfinder, *Planet. Space Sci.*, *48*(15), 1491–1504, doi:10.1016/S0032-0633(00)00097-0.
- Hargraves, R. B. (1959), Magnetic anisotropy and remanent magnetism in hemo-ilmenite from ore deposits at Allard Lake, Quebec, *J. Geophys. Res.*, *64*(10), 1565–1578, doi:10.1029/JZ064i010p01565.
- Hargraves, R. B., D. W. Collinson, R. E. Arvidson, and C. R. Spitzer (1977), The Viking Magnetic Properties Experiment: Primary mission results, *J. Geophys. Res.*, *82*, 4547–4558, doi:10.1029/JS082i028p04547.
- Hargraves, R. B., D. W. Collinson, R. E. Arvidson, and P. M. Cates (1979), Viking Magnetic Properties Experiment: Extended mission results, *J. Geophys. Res.*, *84*, 8379–8389, doi:10.1029/JB084iB14p08379.
- Hecht, M. H., et al. (2008), Microscopy capabilities of the Microscopy, Electrochemistry, and Conductivity Analyzer (MECA), *J. Geophys. Res.*, doi:10.1029/2008JE003077, in press.
- Herkenhoff, K. E., et al. (2003), Athena Microscopic Imager investigation, *J. Geophys. Res.*, *108*(E12), 8065, doi:10.1029/2003JE002076.
- Hviid, S. F., et al. (1997), Magnetic Properties Experiments on the Mars Pathfinder Lander: Preliminary results, *Science*, *278*, 1768–1770, doi:10.1126/science.278.5344.1768.
- Keller, H. U., et al. (2008), Phoenix Robotic Arm Camera, *J. Geophys. Res.*, doi:10.1029/2007JE003044, in press.
- Kletetschka, G., P. J. Wasilewski, and P. T. Taylor (2002), The role of hematite-ilmenite solid solution in the production of magnetic anomalies in ground- and satellite-based data, *Tectonophysics*, *347*, 167–177, doi:10.1016/S0040-1951(01)00243-8.
- Klingelhöfer, G., et al. (2003), Athena MIMOS II Mössbauer spectrometer investigation, *J. Geophys. Res.*, *108*(E12), 8067, doi:10.1029/2003JE002138.
- Kounaves, S., et al. (2008), The 2007 Phoenix MECA Wet Chemistry Laboratory, *J. Geophys. Res.*, doi:10.1029/2008JE003084, in press.
- Madsen, M. B., S. F. Hviid, H. P. Gunnlaugsson, W. Goetz, C. T. Pedersen, A. R. Dinesen, M. Olsen, L. Vistisen, R. B. Hargraves, and J. M. Knudsen (1999), The Magnetic Properties Experiments on Mars Pathfinder, *J. Geophys. Res.*, *104*, 8761–8779, doi:10.1029/1998JE900006.
- Madsen, M. B., et al. (2003), Magnetic Properties Experiments on the Mars Exploration Rover mission, *J. Geophys. Res.*, *108*(E12), 8069, doi:10.1029/2002JE002029.
- Mitrofanov, I., et al. (2002), Maps of subsurface hydrogen from the high energy neutron detector, *Mars Odyssey*, *Science*, *297*, 78–81, doi:10.1126/science.1073616.
- Morris, R. V., D. C. Golden, D. W. Ming, T. D. Shaffer, L. C. Jørgensen, J. F. Bell III, T. G. Graff, and S. A. Mertzmann (2001), Phyllosilicate-palagonitic dust from Mauna Kea Volcano (Hawaii): A mineralogical and process analogue for magnetic Martian dust?, *J. Geophys. Res.*, *106*, 5057–5084, doi:10.1029/2000JE001328.
- Nornberg, P., et al. (2004), Mineralogy of a burned soil compared with four anomalously red Quaternary deposits in Denmark, *Clay Miner.*, *39*, 85–98, doi:10.1180/000985543910122.
- Rieder, R., T. Economou, H. Wänke, A. Turkevich, J. Crisp, J. Brückner, G. Dreibus, and H. J. McSween (1997), The chemical composition of Martian soil and rocks returned by the mobile Alpha Proton X-ray Spectrometer: Preliminary results from the X-ray mode, *Science*, *278*, 1771–1774, doi:10.1126/science.278.5344.1771.
- Rieder, R., R. Gellert, J. Brückner, G. Klingelhöfer, G. Dreibus, A. Yen, and S. Squyres (2003), The new Athena alpha particle X-ray spectrometer for the Mars Exploration Rovers, *J. Geophys. Res.*, *108*(E12), 8066, doi:10.1029/2003JE002150.
- Rochette, P., J.-P. Lorand, G. Fillion, and V. Sautter (2001), Pyrrhotite and the remanent magnetization of SNC meteorites: A changing perspective on Martian magnetism, *Earth Planet. Sci. Lett.*, *190*, 1–12, doi:10.1016/S0012-821X(01)00373-9.
- Sabri, F., T. Werhner, J. Hoskins, A. C. Schuerger, A. M. Hobbs, J. A. Barreto, D. Britt, and R. A. Duran (2008), Thin film surface treatments for lowering dust adhesion on Mars Rover calibration targets, *Adv. Space Res.*, *41*, 118–128, doi:10.1016/j.asr.2007.06.074.
- Smith, P. H., et al. (2008), The Phoenix Mission to Mars, *J. Geophys. Res.*, doi:10.1029/2008JE003083, in press.
- Squyres, S. W., et al. (2003), Athena Mars rover science investigation, *J. Geophys. Res.*, *108*(E12), 8062, doi:10.1029/2003JE002121.
- Toulin, P., III, A. K. Baird, B. C. Cark, K. Keil, H. J. Rose Jr., R. P. Christian, P. H. Evans, and W. C. Kelliher (1977), Geochemical and

mineralogical interpretation of the Viking inorganic chemical results, *J. Geophys. Res.*, 82, 4625–4634, doi:10.1029/JS082i028p04625.

P. Bertelsen, C. S. Binau, L. Djernis Olsen, L. Drube, T. V. Falkenberg, M. P. Haspang, K. Leer, M. B. Madsen, and M. Olsen, Niels Bohr Institute, University of Copenhagen, Blegdamsvej 17, DK-2100 Copenhagen, Denmark. (kleer@fys.ku.dk)

D. Britt, Department of Physics, University of Central Florida, 4000 Central Florida Boulevard, Orlando, FL 32816, USA.

W. Goetz, Max Planck Institut für Sonnensystemforschung, Max-Planck-Str. 2, D-37191 Katlenburg-Lindau, Germany.

M. A. Gross, M. H. Hecht, and C. T. Mogenssen, Jet Propulsion Laboratory, Caltech, Pasadena, 4800 Oak Grove Drive, CA 91109, USA.

M. Lemmon, Department of Atmospheric Science, Texas A&M University, 3150 TAMU, College Station, TX 77843, USA.

J. Marshall, SETI Institute, 515 North Whisman Road, Mountain View, CA 94043, USA.

D. Parrat and U. Staufer, Institute of Microtechnology, University of Neuchâtel, Rue A.-L.-Breguet 2, CH-2000 Neuchâtel, Switzerland.

W. T. Pike, H. Sykulska, and S. Vijendran, Department of Electrical and Electronic Engineering, Imperial College, South Kensington Campus, London SW7 2AZ, UK.

R. Reynolds, A. Shaw, C. Shinohara, P. Smith, R. Tanner, P. Woida, and R. Woida, Lunar and Planetary Laboratory, University of Arizona, 1629 East University Boulevard, Tucson, AZ 85721, USA.